

Nucleon Exchange in the Projectile Fragmentation Reactions
 ^{20}F , ^{20}Ne , ^{20}Na + ^{197}Au and ^{20}F + nat.Ag at 32 MeV/nucleon

D.J. Rowland, R. Ibbotson^a, R. Laforest^b, E. Martin, E. Ramakrishnan^c,
A. Ruangma, M. Veselsky, E.M. Winchester, S.J. Yennello

^a Brookhaven National Laboratory, Brookhaven, NY 11973

^b Mallinckrodt Institute of Radiology, 510 S. Kingshighway, St. Louis, MO 63110

^c Microcal Software, Inc., One Roundhouse Plaza, Northampton, MA 01060

The reactions ^{20}F , ^{20}Ne , ^{20}Na + ^{197}Au and ^{20}F + nat.Ag at 32 MeV/nucleon have been studied at Texas A&M University Cyclotron Institute using the FAUST detector array [1]. The radioactive beams were produced and isolated with the MARS beamline [2]. Projectile fragments were identified in the FAUST array that consists of 68 Si/CsI telescopes covering 90% of the solid angle in the region from 2.31° to 33.63° . Isotopic identification was possible in all detectors for hydrogen and helium and in nearly half the detectors up to $Z = 7$.

The criteria for event selection are two fold for this report. First, on an event-by-event basis the charge of observed fragments in FAUST were summed. The total collected charge was required to be identical to the charge of the beam. The second criteria required that all fragments be isotopically identified.

In the reactions studied, neutrons were not detected. Event reconstruction being dependent on the total collected charge and not on the collected mass enables a study of how the mass of the fragmenting system changes. Even though neutrons were not detected in this experiment, a comparison of model data to the experiment provides insight to the observed mass change of the excited projectile systems.

The mass change of the projectile (ΔN) is defined to be $\Delta N = A_{\text{beam}} - \sum A_{\text{fragment}}$, see Figure 1. Nucleon transfer and evaporation are the two processes that compete to change the original mass of the beams. Nucleon transfer between the target and projectile occurs on a short time-

scale while the two are in contact. The mass of the projectile can be increased by a greater number of nucleons being transferred from the target to the projectile than *visa versa*. Similarly, the mass can be lowered by a greater number of nucleons being transferred from the projectile to the target. Evaporation of nucleons from the projectile will also lead to a lowering of the mass. Since neutrons were not detected, there is no way to determine the balance of transferred neutrons to the loss through evaporation. Therefore ΔN measures the balance between these two processes.

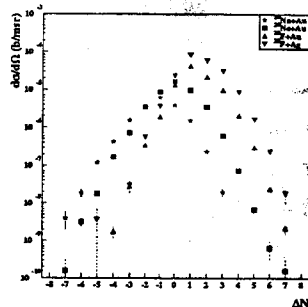


Figure 1: Experimental mass change, ΔN , for the four reactions.

Figure 1 shows that as the isospin of the beam is increased there is a systematic change in peak of ΔN . For ^{20}Na , the lowest isospin, ΔN peaks at -1 (the balance increases the mass by one) and for ^{20}F , the highest isospin, ΔN peaks at 1 (the balance decreases the mass by one).

It is possible to learn something about the competition between these two processes by looking a simulation that reproduces the data accurately. A deep inelastic transfer model (DIT) [3] combined with a statistical

multifragmentation model (SMM) [4] was chosen. Figure 2 shows good agreement of ΔN between the experimental and model data.

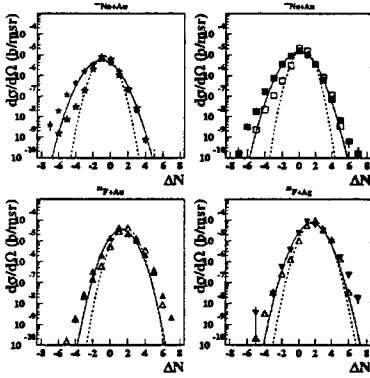


Figure 2: ΔN comparison between the experimental and DIT/SMM model. Experimental data are the solid symbols.

The DIT/SMM model provides more information than what can be obtained in the experiment. At the end of the DIT model, the ^{20}Ne and ^{20}Na projectiles show that on average their masses increase by one after interaction with the target, while for the ^{20}F on average the mass does not change.

After the DIT simulation, SMM is used to breakup the excited projectile. Evaporated neutrons are seen after the multifragmentation stage of the model. The maximum in the distribution is zero for ^{20}Na , one for ^{20}Ne and two for ^{20}F . Combining this with the information from the DIT stage a clearer picture of the observed ΔN arises. The maximum of the DIT mass change for ^{20}F is zero and subtracting from this the number of evaporated neutrons (two for ^{20}F) yields a loss on average of two neutrons which corresponds to an observed $\Delta N = 2$. Doing the same for the ^{20}Ne beam yields an observed $\Delta N = 0$ on average and for ^{20}Na an observed $\Delta N = -1$ on average. For ^{20}Ne and ^{20}Na beams this matches the experimentally observed ΔN . For ^{20}F there is a difference of one nucleon between this model prediction and the experiment, but experimentally $\Delta N = 2$ does

complete closely with $\Delta N = 1$.

Therefore from comparison with the model, a picture emerges in which on average 1, 1 and 0 neutrons are transferred from the target to projectile for ^{20}Na , ^{20}Ne and ^{20}F , respectively. This is then followed by the evaporation of 0, 1 and 2 neutrons on average for ^{20}Na , ^{20}Ne and ^{20}F , respectively.

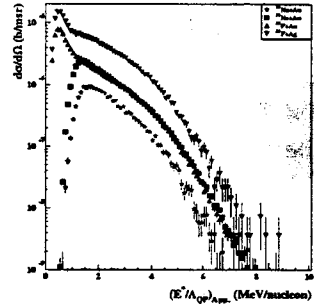


Figure 3: Apparent excitation energy per nucleon as determined from equation 1.

With this information, a more complete excitation energy reconstruction can be performed. Since the experimental setup did not allow for neutron detection, the excitation energy might be better simulated by including any evaporated neutrons. As a first approximation the excitation energy can be calculated as follows:

$$E_{App}^*/A = \left(\sum_i^N (KE + \Delta)_{i,frag} + \Delta_{QP} \right) / A_{QP} \quad (1)$$

where N is the multiplicity of the event, KE is the kinetic energy of the fragments in the center of mass of the Quasi-Projectile (QP), and Δ is the mass excess. Figure 3 shows that the apparent excitation energy distributions of the four reactions are quite similar except at the low end of the spectrum where the Fluorine reactions exhibit a sharp peak. This peak is from multiplicity two events. The ^{20}Ne and ^{20}Na do not have multiplicity two events due to the restriction that all fragments must be identified isotopically. Since the model predicts different amounts of neutron evaporation for the various reactions and that these neutrons are not

detected, the question of whether the excitation energy distributions are similar arises since the excitation reconstruction lacks these missing neutrons.

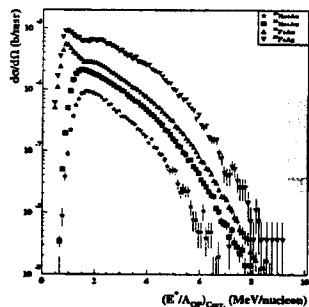


Figure 4: Neutron corrected excitation energy per nucleon spectrum.

Accounting for these neutrons the equation for excitation energy becomes:

$$E_{Corr.}^*/A = \left(E_{App.}^* + \sum_i^{\Delta N} (KE + \Delta)_{i,neutron} \right) / (A_{QP} + \Delta N) \quad (2)$$

where $E_{App.}^*$ from equation 1. The second term in the numerator takes into account $\Delta N > 0$, it is assumed these are evaporated neutrons. The kinetic energy of the neutrons is determined from a Monte Carlo of the proton kinetic energy spectra corrected for the Coulomb peak. This assumption may be an over adjustment but is a first attempt at treating evaporated neutrons. Figure 4 shows the correction and it can be seen that the excitation energy spectra for the four reactions remain similar. Figure 5 shows the comparison of the experimental data to the DIT/SMM code. There is good agreement here, except at the highest excitation energies.

From the comparison of the experimental data to the DIT/SMM model several conclusions can be drawn. First, the DIT/SMM code predicts well the final observed mass change of the QP. This leads to the conclusion that evaporated neutrons need to be taken into account when calculating the excitation energy. The second approximation taken was to add back in ΔN neutrons to the

excitation. Even by doing this the excitation spectra for the four reactions remain alike as shown in figure 4. When comparing the excitation energy spectra between reactions from the model, the distributions for the Fluorine reactions and the Neon reaction are very much alike. The Sodium distribution shows a slightly steeper dependence on the excitation energy. The picture emerges in which the target and projectile transfer several nucleons dissipating kinetic energy into excitation. The final excitation energy distributions of the four reactions seem to have a small dependence on the N/Z ratio of the original projectile.

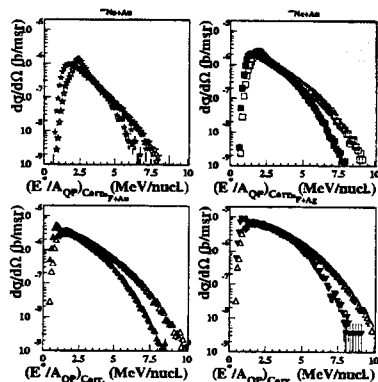


Figure 5: Comparison of experimental and DIT/SMM excitation energy. Experimental data are the solid symbols and the model is represented by the open symbols.

References.

- [1] F. Gimeno-Nogues, *et al.*, Nucl. Inst. and Meth. in Phys. Res. A **399**, 94(1997).
- [2] R.E. Tribble, *et al.*, Nucl. Inst. and Meth. in Phys. Res. A **285**, 441(1989).
- [3] L. Tassan-Got and C. Stéphan, Nucl. Phys. A **524**, 121(1991).
- [4] J.P. Bondorf, *et al.*, Phys. Rep. **257**, 133(1995)